Adenovirus with hexon Tat-PTD modification exhibits increased therapeutic effect in experimental neuroblastoma and neuroendocrine tumors

Di Yu[1], Chuan Jin[1], Justyna Leja[1], Nadim Majdalani[2], Berith Nilsson[1], Fredrik Eriksson[1], Magnus Essand[1]*

[1]Department of Immunology, Genetics and Pathology, Science for Life Laboratory, Uppsala University, Uppsala, Sweden.

[2]Laboratory of Molecular Biology, National Cancer Institute, Bethesda, MD, USA.

***Corresponding author**. Magnus Essand: Department of Immunology, Genetics and Pathology, Uppsala University, SE-75185 Uppsala, Sweden. Phone: +46-18-611 0223. Fax: +46-18-611 0222. Email: magnus.essand@igp.uu.se

Short title: Adenovirus with hexon Tat-PTD modification

Word Count: Abstract, 219 words. Text, 5 671 words

ABSTRACT

Adenovirus serotype 5 (Ad5) is widely used as an oncolytic agent for cancer therapy. However, its infectivity is highly dependent on the expression level of coxsackievirus-adenovirus receptor (CAR) on the surface of tumor cells. Furthermore, infected cells overproduce adenovirus fiber proteins, which are released prior to cell lysis. The released fibers block CAR on non-infected neighboring cells thereby preventing progeny virus entry. Our aim was to add a CAR-independent infection route to Ad5 to increase the infectivity of tumor cells with low CAR expression and prevent the fiber-masking problem. We constructed Ad5 viruses that encode the protein transduction domain (PTD) of the HIV-1 Tat protein (Tat-PTD) in hyper variable region 5 (HVR5) of the hexon protein. Tat-PTD functions as a cell-penetrating peptide and Tat-PTD-modified Ad5 showed a dramatic increased transduction of CAR-negative cell lines compared to unmodified vector. Moreover, while tumor cell infectivity was severely reduced for Ad5 in the presence of fiber proteins it was only marginally reduced for Tat-PTD-modified Ad5. Furthermore, because of the sequence alteration in the hexon HVR, coagulation factor X (FX)-mediated virus uptake was significantly reduced. Mice harboring human neuroblastoma and neuroendocrine tumors show suppressed tumor growths and prolonged survival when treated with Tat-PTD-modified oncolytic viruses. Our data suggests that modification of Ad5 with Tat-PTD in HVR5 expands its utility as an oncolytic agent.

INTRODUCTION

Adenovirus serotype 5 (Ad5), which belongs to the C group of human adenoviruses, has been widely used as an oncolytic agent for cancer therapy (14, 20). Various Ad5 viruses have shown considerable therapeutic effects and have been extensively evaluated in animal models and clinical trials (7, 22, 27, 30, 44). Their advantage in cancer therapy is due to the self-propagation properties that involve replication in and lysis of infected tumor cells, which leads to secondary infection and killing of adjacent cells within the tumor. However, one limiting factor for Ad5 efficacy in cancer therapy is that the infection is dependent on coxsackievirus-adenovirus receptor (CAR) expression on target cells. CAR is an adhesion molecule expressed in tight-junctions and many cancer cells down-regulate CAR expression, which results in difficulties in achieving sufficient infection and, as a consequence, the oncolytic therapeutic effect is hampered (39). One approach to circumvent this is to genetically modify Ad5 and use fibers or fiber knobs from the B group of adenoviruses, which do not bind to CAR but to other cell surface receptors (48, 49). A second limiting factor is fiber-masking of receptors. This is caused by overproduction of adenovirus fiber proteins (4, 17, 31), which are released from the infected cell before cell lysis. The released fibers bind to CAR on non-infected neighboring cells, thereby limiting infection efficiency of progeny virus (31). The fiber-masking problem is not limited to the Ad5 fiber but was also observed for the Ad35 fiber, which binds to CD46 (31). These limitations must be overcome to develop successful oncolytic adenovirus agents.

Cell penetrating peptides (CPPs) have been intensively studied and widely used to deliver cargos into cells regardless of cellular specificity and independent of cell surface receptor expression. Drug delivery with CPPs has also been used in preclinical models and clinical trials (12, 35). Kurachi et. al. generated a recombinant adenovirus with the protein transduction domain (PTD) of the HIV-1 Tat protein (Tat-PTD) inserted into either the HI loop or the C-terminus of the viral fiber (23). Both modifications resulted in elevated transgene expression compared with unmodified virus. However, although such an oncolytic virus can overcome CAR-dependency it still uses the fiber for infection and the excess production of fibers may block the uptake of progeny virus in neighboring cells. Eto et. al. showed that adenoviruses where Tat-PTD was chemically conjugated to lysine residues on the capsid proteins, such as the adenovirus hexon, fiber, and penton base proteins, expanded the virus tropism to CAR-negative cell lines (15). While this may be an excellent approach to expand the tropism of adenoviral vectors it is not useful for oncolytic viruses, which rely on production of progeny virus for further rounds of infection. Only the initial virus contains the Tat-PTD modification and the progeny virus is not equipped to overcome CAR-dependency and fiber-masking.

Here we genetically introduce the Tat-PTD sequence on hyper variable region 5 (HVR5) of the hexon protein, the major coat protein of the virus capsid, to add a CAR independent route of infection. We found that Tat-PTD-modified Ad5 vectors could transduce CAR-negative neuroendocrine tumor cells and that efficacy of Tat-PTD-modified oncolytic Ad5 viruses were increased *in vitro*, which resulted in an improved therapeutic effect *in vivo*. We also found that Tat-PTD-modified oncolytic Ad5 was not

84 blocked by soluble Ad5 fibers to the same extent as non-modified Ad5 and that it yields
85 larger plaques, indicating that the Tat-PTD-modified Ad5 is able to overcome the fiber-
86 masking problem.
87

MATERIALS AND METHODS

Cell lines

All cell culture reagents were purchased from Invitrogen (Carlsbad, CA) except when mentioned otherwise. Cell cultures were maintained in 95% humidity incubator with 5% CO_2 atmosphere at 37°C. The cell lines BON (a kind gift from Prof. J.C. Thompson and Prof. C.M. Townsend, Galveston, TX), CNDT2.5 (13, 43) (a kind gift from Prof. L.M. Ellis, MD Anderson, Houston, TX), SKOV-3 (ATCC, Manassas, VA), A549 (ATCC), MB49, 911 (Crucell, Leiden, The Netherlands), 1064SK, mel526 (a kind gift from Prof. T. Boon, LICR, Brussels, Belgium) were cultured as described elsewhere (28). The human neuroblastoma cell line SK-N-SH (a kind gift from Dr. F. Hedborg, Uppsala University, Uppsala, Sweden) was cultured in MEM supplemented with 10% FBS, 1mM NaPyr, PEST. The human umbilical vein endothelial cell line HuVec (3H Biosciences, Uppsala, Sweden) was cultured in Endothelial Cell Growth Medium MV2 supplemented with 5ng/mL hEGF, 0.5ng/mL hVEGF, 20ng/mL R3 IGF, 200ng/mL Hydrocortisone, 10ng/mL hbFGF, 1µg/mL Ascorbic Acid (PromCell, Heidelberg, Germany). The Rmcb hybridoma cell line, which secrete anti-CAR antibodies, was purchased from ATCC and maintained in RPMI-1640 supplemented with 10% FBS.

Flow cytometry

The CAR expression level on the cell lines were assessed by flow cytometry as described elsewhere (28).

Recombinant adenoviruses construction by λ-Red recombineering

All recombinant adenovirus outlined in Figure 1a were generated based on λ-phage mediated-recombineering in E. *coli* strain SW102 using bacmid pAdZ5-CV5-E3+ (kindly provided by Dr. Richard Stanton, Cardiff University, Cardiff, UK) (38). This bacmid contains the adenovirus serotype 5 genome, with the E1 region replaced by a selection/counter-selection cassette (*als* cassette) consisting of the *bla* (ampicillin resistance), *lac*Z (beta galactosidase) and *sac*B (sucrose resistance) genes. To generate pAd5(GFP), the CMV-GFP cassette was PCR amplified from Ad5(GFP) (28) using primers pF.Shuni and pR.Shuni and purified by gel extraction. Heat activated and freshly made competent E. *coli* SW102 cells containing pAdZ5-CV5-E3+ were electroporated with 100ng PCR product using Gene Pulser II (Bio-Rad Laboratories, Hercules, CA). Selection was performed on LB-sucrose plates, containing LB without NaCl, 6% sucrose, 200µM of isopropylthio-β-galactoside (IPTG, Sigma-Aldrich, St. Louis, MO) and 40µg/ml of 5-bromo-4-chloro-3-indolyl β-D-galactopyranoside (X-Gal, Invitrogen). Positive colonies were designated pAd5(GFP).

To generate a scar-free modification in hexon HVR5, the selection/counter-selection method was used. The general procedure is described in Figure 1a. Briefly, the *als* cassette was PCR amplified using primers pF.HVR5-*als* and pR.HVR5-*als* and knocked in into the HVR5 site in pAd5(GFP). Selection was performed on LB agar plates containing 100µg/ml of Ampicillin, 200µM of IPTG and 40µg/ml of X-Gal. Positive colonies were designated pAd5(GFP, HVR5^{als}). Next, the *als* cassette was replaced by the Tat-PTD motif to generate pAd5PTD(GFP). Selection was performed on LB-sucrose plates.

The Tat-PTD motif fragment was generated by joint-PCR with primer pairs pF1.HVR5-PTD/pR1.HVR5-PTD and pF2.HVR5-PTD/pR2.HVR5-PTD.

pAd5PTD(wt) and pAd5PTD(D24) were generated in the same manner by replacing the CMV-GFP cassette from the E1 region with serotype 5 wildtype E1A-E1B or E1A(D24)-E1B sequences. The *als* cassette was amplified using primers pF.E1-als/pR.E1-als to replace the CMV-GFP cassette. pF.Shuni and pR.Shuni were used for amplification of either the E1 region from wild type adenovirus DNA or E1-D24 region from plasmid AdEasy(D24).fk3 (a kind gift from Prof. A. Hemminki, Helsinki University, Helsinki, Finland). The PCR products were then used for replacement of the *als* cassette in the E1 region to generate pAd5PTD(wt) and pAd5PTD(D24) respectively. The viruses generated from pAd5PTD(GFP), pAd5PTD(wt) and pAd5PTD(D24) were named Ad5PTD(GFP), Ad5PTD(wt) and Ad5PTD(D24). A predicted (24) model of the trimerized hexon with Tat-PTD in HVR5 based on published hexon structure (33) (PDB: 1P30) is presented in Figure 1b. All viruses used in this study are described in Figure 1c. All primers used can be found in Table 1.

Virus production and titration

Wild-type Ad5 (ATCC) was propagated in A549 cells, while all other genetically modified viruses were propagated in 911 cells (16). The replication-defective E1/E3-deleted AdMock, herein called Ad5(mock), has been described earlier (6). All viruses were purified by CsCl gradient ultracentrifugation, dialyzed against a viral storage buffer

(10mM Tris-HCL pH8.0, 2mM MgCl2, 4%(w/v) sucrose) as described (7, 26) and stored in aliquots at -80°C.

Since the viral surface protein was modified in this study, the infectious virus titer will depend on cell line used for titration. Therefore, virus titers (encapsidated viral genomes) were determined by real time quantitative-PCR (40). Briefly, viral DNA was extracted using High Pure Viral Nuclear Acid Kit (Roche, Mannheim, Germany). DNA copy number was detected using primers Ad.titration.F and Ad.titration.R targeting the adenovirus E4 orf1 region. Plasmid, pCR2.1(AdE4orf1), containing the same amplicon was used for the generation of standard curve (10). Virus titer was calculated as mean of three independent experiments. The titer was designated as encapsidated viral genome (evg). A fluorescent forming unit (FFU) assay on 911 cells was also used to determine the infectious virus titers (9). The evg/µl, FFU/µl and evg/FFU ratios of the viruses used in this study are given in Figure 1d. We used fixed evg when comparing the viruses on the various cell lines.

Transduction efficiency assay

Cells were de-attached and mixed with appropriate amount of GFP-containing virus at different evg/cell at 37°C for 2 hours in a volume of 200µL. Free virus was washed away after transduction and cells were seeded in 24-well plates. The percentage of GFP-expressing cells was evaluated by flow cytometry (FACSCalibur, BD Biosciences, Franklin Lakes, NJ) after 48 hours.

Cell viability assay

Cells were transduced with virus in suspension for 2 hours with different evg per cell and then seeded in a 96-well plate in a total volume of 100μL (1000 cells/well for SK-N-SH and 5000 cells/well for CNDT2.5). Cell viability was evaluated at day 4 using MTS Cell Titer Aqueous One Solution Cell Proliferation Assay Kit (Promega, Madison, WI). The relative cell viability was calculated using the ratio between the average absorbance for viral transduced cells and the average for non-transduced cells.

In vitro viral replication assay

Cells were seeded in 24-well plates to 80% confluency and transduced with virus at 500 evg per cell. The transduction medium was replaced by cell culture medium after 2 hours. Viral genomic DNA was isolated directly after transduction (day 0) and at days 1, 2, 3 and quantified by real-time PCR. Relative viral replication was present as the fold-increase of genomic DNA copy number.

Western blot

SK-N-SH cells were transduced in suspension with Ad5PTD(GFP), Ad5(wt), Ad5PTD(wt) and Ad5PTD(D24) at 500 evg/cell and cultured in 12-well plates. Cells were harvested 48 hours later and total protein extracts were prepared, E1A and β-actin protein expression were detected as described before (26) with minor modifications. In brief, the membrane was incubated with a mouse monoclonal anti-E1A antibody (M73, Neomarkers Inc., CA) and a goat polyclonal anti-β-actin antibody (Santa Cruz

Biotechnology, Santa Cruz, CA). After washing, the membrane was incubated with a rabbit-anti-mouse-680 antibody (Invitrogen) and donkey-anti-goat-800 antibody (Odyssey Infrared Imaging, LI-COR Biosciences, Lincoln, NE). The membrane was then scanned using the Odyssey Infrared Imaging System (LI-COR Biosciences).

Fiber blocking assay

Soluble Ad5 fiber molecule was obtained as described (31). A549 cells were transduced at 500 evg/cell with Ad5(GFP) or Ad5PTD(GFP) in the presence or absence of fiber molecules (500µL) for 2 hours. Cells were then washed once and seeded in a 24-well plate. After 48 hours GFP-expressing cells were analyzed by flow cytometry.

Plaque formation assay

A standard plaque formation assay with neutral red staining as described (42) was performed to visualize plaques. In brief, monolayer A549 cells in a six-well plate were transduced with 100 evg of either Ad5(wt) or Ad5PTD(wt). The medium was removed and the cells were washed once with PBS and overlayed with low-melting agar. After 5 days the cells were once more overlayed with low-melting agar containing neutral red (Sigma) for visualization of plaques and the plates were thereafter inspected daily. Plaques were measured on day 8 after viral transduction using an eyepiece graticule and visualized by scanning the plate.

Factor X-mediated adenovirus binding assay

SKOV3 cells were plated in a 24-well plate at 1×10^5 cells/well. The next day, the cells were incubated with virus in the presence or absence of the physiological level of coagulation factor X (FX, 8μg/mL) (Haematologic Technologies Inc., Essex Junction, VT) at 500 evg/cell in a total volume of 300μL at 4°C for 1 hour while rocking. Thereafter, the supernatant was replaced by cell culture medium. Viral genomic DNA was isolated directly after incubation using High Pure Viral Nucleic acid kit (Roche) and quantified by real-time PCR as described above for virus titration.

Either Ad5(wt) or Ad5PTD(wt) were mixed with reactive fluorescein isothiocyanate (FITC) at a ratio of 1ug FITC per 1×10^{10} evg viruses in borate buffer (pH=9.0) and incubated for 1 hour at 37 °C. The FITC-labeled viruses were then dialysed against PBS. Real-time measurements of the binding of FITC-labeled viruses to SKOV3 cells was performed at room temperature in LigandTracer® Green (Ridgeview Instruments AB, Uppsala, Sweden), essentially according to a previously published protocol (3). Compare to surface plasma resonance, LigandTracer Green is an alternative instrument for monitor virus-cell interaction. Briefly, a baseline was generated by incubation of cells in 3ml of culture medium. The cells were then incubated for approximately 2 hours with 5000 evg FITC-labeled viruses in the presence or absence of FX (8μg/mL) while the association rates were recorded. After incubation, the virus solution was replaced with fresh medium and the dissociation rate was followed and recorded.

Neutralization assay

Neutralizing antibody was prepared by immunizing mice with adenovirus followed by isolation of plasma from whole blood. Briefly, Balb/c mice were injected intraperitoneally (i.p.) with Ad5(mock) at 1×10^{10} evg/mouse and boosted twice with the same amount of virus with 2 weeks intervals. Plasma was isolated from whole blood by centrifugation at 3000×g for 20 min at 4°C. The plasma was heat inactivated at 56°C for 1 hour. Ad5(GFP) and Ad5PTD(GFP) were then mixed with plasma dilutions (1:10 to 1:1,000,000) in a 96-well plate at 1×10^{6} evg with a volume of 100µL/well. The plate was incubated at 37°C for 1 hour. Subsequently, 1×10^{5} 911 cells were added in a volume of 100µL to each well. After 24 hours incubation, cells were analyzed for GFP expression by flow cytometry (BD LSR II Flow Cytometer, BD sciences).

Animal studies and tumor models

Female, SCID/beige mice, 3-4 weeks old were purchased from Taconic (Denmark). Male, NMRI-nude mice, 3-4 weeks old were purchased from Harlan (Germany). All mice were housed at the Rudbeck animal facility (Uppsala, Sweden) in individually ventilated cages (3 mice per cage). Tumor implantation was performed 1 week after mice delivery.

Neuroblastoma cells (1×10^{6} SK-N-SH) were mixed 1:1 (v/v) with Matrigel (BD Biosciences) in a total volume of 50µL and injected subcutaneously in the hind flank of SCID/beige mice. Mice were treated with peritumoral injections of either Ad5(wt), Ad5PTD(wt), Ad5PTD(D24) or PBS on days 10, 12, 14 and 16 at a dose of 5×10^{9} evg/injection in 30µL. Six mice per group were used. Tumor growth was monitored by caliper measurement. Tumor size was calculated using ellipsoid volume formula (Length

263 × Width × Depth × π / 6). The experiment was terminated directly after the last mouse
264 was sacrificed in the Ad5(wt)-treatment group.

265 Neuroendocrine tumor cells (5×10^6 CNDT2.5) were mixed 1:1 (v/v) with Matrigel
266 (BD Biosciences) in a total volume of 100µL and injected subcutaneously in the hind
267 flank of NMRI-nude mice. Mice were treated with intratumoral injections of either
268 Ad5(mock), Ad5PTD(D24) or PBS on days 17, 19, 21 and 23 at a dose of 5×10^9
269 evg/injection in 30µL. Six mice per group were used. Tumor growth was monitored by
270 caliper measurement. Tumor size was calculated using ellipsoid volume formula (Length
271 × Width × Depth × π / 6).

272

273 **Statistical analysis**

274 Statistical analysis was performed using the GraphPad Prism software version 5.01
275 (GraphPad Software, San Diego, CA). Unpaired Student's *t*-test was used to compare the
276 transduction efficiency, MTS cell killing assay, viral replication assay, fiber blocking assay,
277 anti-CAR antibody blocking assay and neutralization assay. Mann-Whitney test was
278 performed to compare plaque sizes in plaque formation assay. Log-rank test was used to
279 compare survival curves created by the Kaplan-Meier method. Tumor sizes in different
280 treatment groups were compared using two-way ANOVA.

281

282 **Biosafety level and ethics declaration**

283 The Swedish Work Environment Authority has approved the work with genetic
284 modification of the infectious capacity of human adenovirus serotype 5 (ID number

202100-2932 v66a13 (laboratory) and v66a9 (mice)) and genetic modification of replication capacity of human adenovirus serotype 5 (ID number 202100-2932 v66a11 (laboratory) and v66a7 (mice)). All experiments regarding modified adenoviruses were conducted under Biosafety level 2. The Uppsala Animal Ethics Committee has approved the animal studies (ID number C319/9).

RESULTS

A Tat-PTD-modified adenoviral vector can efficiently transduce CAR-negative cells.

Adenoviral vectors are widely used as gene transfer vehicles. They efficiently introduce foreign genes into cells expressing CAR, the native receptor for Ad5 infection. Here we compared the gene transduction capacity of two GFP-expressing adenoviral vectors in a range of cell lines. Ad5(GFP) use the same infection route as wild-type Ad5 while Ad5PTD(GFP) in addition to the Ad5 infection route has the Tat-PTD sequence in HVR5 of the hexon protein on the virus capsid. SK-N-SH, MB49, CNDT2.5 and 1064SK are CAR-negative or have low CAR expression levels, whereas A549, mel526, HuVec, BON express moderate to high levels of CAR (**Figure 2**). Ad5PTD(GFP) showed efficient transduction of CAR-negative cell lines while Ad5(GFP) showed no or very poor transduction of these cells (**Figure 2**). Furthermore, transduction of CAR-positive cell lines by Ad5PTD(GFP) was always more efficient or as efficient as transduction with the unmodified Ad5(GFP) (**Figure 2**). These results indicate that insertion of a small cell penetrating peptide into the adenoviral hexon protein surface HVR5 region dramatically enhances adenovirus transduction ability.

Tat-PTD-modified oncolytic adenoviruses yield enhanced cell killing.

Genetically engineered oncolytic adenoviruses have been tested in several clinical cancer trials. Therefore, we wanted to investigate whether the oncolytic ability of Ad5 could be enhanced by the Tat-PTD modification. Two replication competent Tat-PTD-modified adenoviruses were produced. Ad5PTD(wt) is a wild type adenovirus with Tat-

PTD in HVR5, and Ad5PTD(D24) is a Tat-PTD-modified virus with a 24bp deletion in E1A, which confers selectivity to replication in pRb pathway-deficient cancer cells (2, 19). *In vitro* cell killing and viral replication assays were performed. The Ad5PTD(wt) and Ad5PTD(D24) viruses exhibited significantly ($p<0.001$ at 1000 evg/cell) increased killing ability of CAR-negative neuroblastoma and neuroendocrine tumor cells compared to un-modified wild type virus Ad5(wt) (**Figure 3a**). Furthermore, Ad5PTD(wt) and Ad5PTD(D24) yielded significantly ($p<0.001$ at day 3) higher numbers of progeny virus compared to Ad5(wt) (**Figure 3b**). The increased cell killing and replication are tributes to higher transduction efficacy. Interestingly, Ad5(wt) did replicate in SK-N-SH cells to a certain degree but did not exhibit any killing ability in this cell line, not even at 1000 evg/cell, most likely due to the inability to achieve a high enough transduction level of these cells (**Figures 3a,b**), while the Tat-PTD-modified viruses showed both killing and replicating activities (**Figures 3a,b**). Western blot analysis detects E1A protein expression in SK-N-SH cells only after transduction with the Tat-PTD-modified viruses, indicating once more that the transduction rate of wild type Ad5 is very low in this cell line (**Figure 3c**). These results show that the Tat-PTD modification can broaden the viral transduction ability with gain in killing of CAR negative cells and without any loss of oncolytic capacity in CAR-positive cells (data not shown).

Tat-PTD-modified adenovirus overcomes the fiber-masking problem leading to increase in oncolytic virus spread.

The adenovirus fiber protein is expressed in huge excess during the cycle of viral infection-replication (4, 17, 31). Recently, it was reported that the excess fiber proteins, which are released to the environment before mature viral particles lyse the infected cells, masks the receptors on uninfected cells in the vicinity thereby preventing the second round of progeny virus infection (31). This property hampers the spread of oncolytic virus within tumors. Since the Tat-PTD-modified virus has a CAR-independent entry mechanism, we compared gene transfer activity of Ad5(GFP) and Ad5PTD(GFP) in the presence of excessive soluble fiber molecules. GFP expression in cells transduced with Ad5(GFP) in the presence of soluble fiber was reduced to 20% compared to that in the absence of soluble fiber. However, cells transduced with Ad5PTD(GFP) retained 80% transduction efficacy in the presence of soluble fiber (**Figure 4a**). Furthermore, we performed a plaque formation assay to evaluate virus spread during replication. The plaques formed by Ad5PTD(wt) started to be visible at day 3, while the plaques formed by Ad5(wt) started to be visible at day 6. At day 8, the plaques formed by Ad5PTD(wt) was on average 1.6 times larger in average than the plaques formed by Ad5(wt) (**Figure 4b**). A representative data set of the plaques formed by both viruses is shown in **Figure 4c** with entire wells shown in the upper panel and photographs with 10× magnification pictures of the plaques shown in the lower panel. These results indicate that viruses with the Tat-PTD-modification can overcome the fiber-masking problem and thus enhance the second round of infection by progeny virus. Moreover, these results further strengthen the notion that the Tat-PTD-modified virus can enter the cells via a CAR-independent pathway.

Tat-PTD-modified Ad5 vector can resist FX-mediated uptake and partially overcome anti-Ad5 antibody neutralization.

It has been reported that viral transduction of hepatocytes is mediated by binding of coagulation factor X (FX) to the hypervariable region of the Ad5 hexon surface (47). We investigated whether our Tat-PTD-modification could reduce the FX-mediated viral uptake by incubating SKOV3, a cell line commonly used to demonstrate FX-mediated Ad5 uptake, with or without physiological concentrations of FX. By real-time measurements of virus-cell interactions using Ligand Tracer®, we found that FITC-labeled Ad5PTD(wt) showed far less FX-mediated binding to SKOV3 cells than FITC-labeled Ad5(wt) during the retention phase (**Figure 5a**). These results were confirmed by real-time quantitative PCR measurement of viral genome copies associated with the cells after binding. For the real time PCR experiments, the viral binding ability of the unmodified Ad5(GFP) vector was about 20 times higher than the binding of the Tat-PTD-modified Ad5PTD(GFP) vector to the cell surface of SKOV-3 cells in the presence of FX (**Figure 5b**). Taken together, these results indicate that the small modification of introducing Tat-PTD in HVR5 significantly altered FX-mediated viral uptake.

One limitation of using oncolytic adenovirus for cancer virotherapy is the high prevalence of neutralizing anti-Ad5 antibodies (32), which may limit the use of intravenous administration of Ad5. We investigated whether the Tat-PTD modification conferred the ability to escape from existing neutralizing antibodies (NAbs). Mice were immunized with unmodified Ad5. Plasma was isolated from the immunized mice and

used to perform *in vitro* neutralization assay. Tat-PTD-modified viruses were moderately protected from NAbs. There was a trend towards protection for all plasma dilution points but only two points reached statistically significant differences (**Figure 5c**).

Treatment with Tat-PTD-modified oncolytic adenoviruses delays tumor growth and prolongs survival in mice carrying xenografted human neuroblastoma and neuroendocrine tumors.

To evaluate the oncolytic viruses as therapeutic agents *in vivo*, SCID/beige mice harboring human neuroblastoma (SK-N-SH), and NMRI-nude mice harboring human neuroendocrine tumors (CNDT2.5) were used. Tumor cells were implanted subcutaneously on the right hind flank. Once established, SK-N-SH tumors on SCID/beige mice were treated with peritumoral injections of Tat-PTD-modified viruses or Ad5(wt) while PBS was used as control. CNDT2.5 tumors on NMRI-nude mice were treated with intratumoral injections of Ad5PTD(D24) while Ad5(mock) and PBS were used as controls. Tumor growth was monitored by caliper measurements.

In the SK-N-SH xenograft model, mice treated with either Ad5PTD(wt) or Ad5PTD(D24) showed a significant ($p<0.001$) suppression of tumor growth (**Figure 6a**) and prolonged survival compared to mice treated with Ad5(wt) (**Figure 6b**). Interestingly, there was no difference between Ad5(wt)-treated mice and PBS-treated mice, reflecting the lack of Ad5(wt) transduction of SK-N-SH cells.

In the CNDT2.5 xenograft model, mice treated with Ad5PTD(D24) showed a significant ($p<0.001$) suppression of tumor growth compared to mice treated with the

400 replication-defective virus Ad5(mock) or PBS (**Figure 6c**). Although, there was a
401 significant tumor growth suppression for Ad5(mock)-treated mice compared to PBS-
402 treated mice, no mice were cured in the Ad5(mock)-treatment group. Moreover, mice
403 treated with Ad5PTD(D24) showed a significantly prolonged survival compared to PBS-
404 treated mice and Ad5(mock)-treated mice and in addition, two mice out of six were
405 cured by the Ad5PTD(D24) treatment (**Figure 6d**). The better results for Ad5PTD(D24)
406 compared to Ad5(mock) is most likely a combination of the PTD modification, D24
407 deletion of E1A and the fact that Ad5PTD(D24) replicates while Ad5(mock) does not.
408

DISCUSSION

Adenoviruses are widely used for gene transduction and oncolytic therapy. In order to selectively target certain cell types, many groups, including our own, have modified the viral capsid or fiber protein (8, 22, 28, 44). Most studies report modifications of either the HI loop or the C-terminus of the adenovirus fiber. However, tumor selectivity can also be achieved by promoter-controlled E1A expression in tumor tissues or micro RNA target sequences to selectively degrade E1A expression in off-target tissues (7, 26, 27). The main aim of this study was to increase viral transduction efficiency and to overcome the fiber-masking problem caused by excessive fiber proteins release from infected cells that blocks CAR on non-infected neighboring cells and prevents progeny virus entry (31). To achieve this, we decided to keep the targeting agent away from the fiber and to put it on the virus capsid. Although modification of the hexon HVR has been difficult to achieve (50) several groups have verified that the HVR5 site is tolerant for foreign peptide insertion (37, 45, 46, 50). Moreover, given the fact that there are 240 hexon trimers expressed on the adenoviral surface versus only 12 fiber trimer molecules and that hexon modification would not affect the native fiber binding, we decided to modify the hexon HVR5 site.

Our targeting peptide of choice is the protein transduction domain of the Tat protein from HIV-1 (Tat-PTD). Kurachi et. al. have previously introduced Tat-PTD in the adenovirus fiber knob (23) and Eto et. al. reported a method to modify adenovirus with Tat-PTD by chemical conjugation to lysine residues on exposed viral proteins (15). However, the chemical conjugation procedure is relatively complex and the exact ratio

431 of conjugated Tat-PTD peptide per viral particle could not be determined (15, 51). In our
432 case, the Tat-PTD sequence was flanked by a short α-helix spacer and genetically
433 inserted into the hexon HVR5 region. We hypothesized that the short α-helix spacer
434 would expose the Tat-PTD motif, thereby increasing the virus-cell interactions, thus
435 improving the transduction efficiency. The predicted model of the modified trimerized
436 hexon (**Figure 1b**) was obtained by superimposition of the Tet-PTD and linkers on the
437 hexon trimer previously modeled by others. It shows that the Tat-PTD sequence in HVR5
438 is exposed on the top surface of the hexon, the portion of the protein facing the
439 surrounding.

440 The transduction efficiency of Ad5PTD(GFP) was dramatically increased for CAR-
441 negative cell lines compared to the unmodified virus Ad5(GFP). Interestingly, up to 90%
442 of the SK-N-SH cells, which are non-permissive for native adenovirus transduction, could
443 be transduced by the Tat-PTD-modified Ad5PTD(GFP). In all other tested cell lines, the
444 modified vector shows the same or better transduction efficiency than the non-
445 modified Ad5(GFP) vector. The mechanism of cellular uptake and cell penetration of
446 CPPs has been studied for decades and still remains divergent. Different models have
447 been proposed to describe the mechanism. In general, these models can be categorized
448 as energy-dependent endocytosis and direct translocation via the lipid bilayer (34).
449 Another suggestion is that CPPs only play a role in “adherence” or “docking” to the cell
450 surface while endocytosis mediates the actual cellular uptake (25). The secondary
451 structure was also found to be important for different classes of CPPs (11). In our case,
452 the exact transduction mechanism of the Tat-PTD modified viruses is unclear. We are

able to transduce CAR-negative cells with the Tat-PTD-modified viruses and the transduction can only be partly blocked by soluble fiber molecules, which strongly indicates that a CAR-independent pathway is utilized for cellular uptake.

Recent data have demonstrated that the over-produced fiber molecules during the first round of viral infection is released prior to cell lysis and mask the receptor on adjacent uninfected cells and therefore inhibit the following rounds of infection (31). This phenomenon limits the usage of replicating oncolytic adenoviruses as anti-cancer agents. In contrast to chemically conjugated Tat-PTD-modified virus (15) or HI-loop/C-terminus Tat-PTD-modified virus (23), which would only enhance the first round of infection, we show that our Tat-PTD-modified virus, which utilizes a CAR-independent cellular transduction pathway, can overcome this problem. The plaque formation assay confirmed that Ad5PTD(wt) spreads faster than Ad5(wt) in a 2-dimensional model, which implicates that the Tat-PTD-modified virus should spread faster also in 3-dimentional structural tumors.

Hexon proteins were reported to play a major role in liver toxicity after intravenous administration of adenovirus (47). Liver infection, at least in mice, is mediated by binding of FX (Gla domain) to the hypervariable region of the Ad5 hexon surface. The uptake of FX-Ad5 complexes in hepatocytes is mediated through a heparin-binding exosite in the FX serine protease domain. It has also been demonstrated that a single mutation on HVR5 or HVR7 could significantly reduce or totally abolish the FX binding ability (1). We evaluated the FX de-targeting ability of our HVR5 modified virus. Consistent with other reports, we found that the substitution of HVR5 by the Tat-PTD

motif significantly reduces the FX mediated virus cellular binding activity in two independent assays. In addition, the modification of the hexon removes antigenic epitopes on the virus particle surface, which lead to partial protection from pre-existing neutralizing anti-Ad5 antibodies. Surprisingly, the protection from NAbs was not as efficient as was reported for the Tat-PTD chemically conjugated viruses (15) and the other hexon-modified viruses (32, 36). This is probably due to that the relatively small-sized modification cannot remove all natural Ad5 viral capsid epitopes.

We also examined the *in vivo* therapeutic effects of the Tat-PTD-modified oncolytic viruses on human neuroblastoma and neuroendocrine tumors. To our knowledge, this is the first study using adenoviruses modified with cell-penetrating peptides as oncolytic agents for cancer therapy. The human neuroblastoma cell line SK-N-SH was chosen for establishing xenografts since it is not transducable by native Ad5. We found that therapeutic effect on SCID/beige mice with SK-N-SH xenografts can only be achieved by treatment with Tat-PTD-modified viruses, indicating that viral entry is crucial in order to achieve an oncolytic therapeutic effect. Since Ad5PTD(wt) is not tumor selective we also produced and evaluated the Ad5PTD(D24) virus along with Ad5(wt) and Ad5PTD(wt). We found that Ad5PTD(D24) is as efficient as Ad5PTD(wt), but not better (**Figure 6a, b**). Therefore, only Ad5PTD(D24) was selected for treatment of neuroendocrine CDNT2.5 tumors on NMRI-nude mice. Geoerger *et. al*. reported on an adenovirus AdΔ24-425S11 expressing a bispecific scFv which targets both the adenoviral fiber knob and the epidermal growth factor receptor, to generate higher transduction level on CAR-low neuroblastoma cells (21). However, the infectivity-enhancement of

497 that virus still relies on uptake via CAR at the first round of viral infection in order to
498 produce the 425S11-targeting adapter. In contrast, the infectivity of our Tat-PTD-
499 modified viruses is guaranteed also on CAR-low cells at the first viral infection step and
500 will be carried on to viral progeny. Parikh *et. al*. claimed that treatment of
501 neuroblastoma by wild-type Ad5 was not as efficient as by oncolytic herpes simplex
502 virus due to the lack of Ad5 transduction (29). We show in this study that by enhancing
503 Ad5 transduction, therapeutic effect could be achieved for neuroblastoma.

504 It has been reported that the therapeutic effect achieved by treatment with
505 oncolytic virus is partially dependent on the host immune response raised by viral
506 infection (5, 41, 52). We evaluated the therapeutic effect on both a nude and a
507 SCID/beige mouse models. Nude mice, lacking T cells but with functional B and NK cells,
508 reflect the therapeutic effect from both viral oncolysis and a partially functioning host
509 immune system. SCID/beige mice, deficient for T, B and NK cells, are severely immuno-
510 compromised, thus any therapeutic effect observed is solely dependent on viral
511 oncolytic activity. Nude mice harboring CNDT2.5 xenografts treated with Ad5(mock)
512 showed delayed tumor growth, indicating that a virally induced host immune response
513 was involved. SCID/beige mice have also reported to have dysfunctional platelets and
514 therefore prolonged bleeding time after needle puncture (18). All the SCID/beige mice
515 harboring tumor xenografts got wounds in the tumor area during tumor growth,
516 therefore the experiment had to be terminated immediately after the last mouse in the
517 Ad5(wt)-treatment group was sacrificed.

The changed tropism caused by genetic introduction of Tat-PTD in the Ad5 hexon raises potential safety concerns since the virulence and pathogenicity/transmission in the natural host as well as the host range may have changed. It is therefore important to combine the transductional alteration caused by Tat-PTD with a transcriptional modification in order to restrict virus activity in normal cells. In this paper we chose to combine it with the D24-deletion of E1A. An alternative approach would be to control E1A gene expression with a tissue- or tumor-specific promoter. In either case, the safety and virulence of Tat-PTD-modified Ad5 will have to be further examined and monitored before a clinical trial can be proposed. It should however be noted that neutralizing Ad5 antibodies are quite efficient in neutralizing also Tat-PTD-modified Ad5. Ad5PTD(wt) shows significantly better shielding against Ad5 Nabs only under certain dilutions of sera (1:1250-1:625). This means that under physiological conditions, Ad5 NAbs in the blood stream will neutralize Tat-PTD-modified Ad5. Nevertheless, it is very important to follow strict guidelines when working with Tat-PTD-modified replicating viruses.

In conclusion, we have developed Tat-PTD-modified oncolytic Ad5-based viruses with elevated infectivity. The viruses circumvent problems caused by excessive production and secretion of virus fiber protein in the first round of infection, fibers that could block receptors on neighboring non-infected cells and slow down subsequent replication rounds. They are particularly promising for the treatment of tumors with low CAR expression as demonstrated herein for experimental neuroblastoma and neuroendocrine tumors.

ACKNOWLEDGEMENTS

We are grateful to Richard Stanton (Cardiff University, Cardiff, UK), Don Court (National Cancer Institute, Frederick, MD), Bhupender Singh and Linda Sandin (Uppsala University, Uppsala, Sweden), Ann-Charlotte Hellström (Alligator Bioscience AB, Lund, Sweden), Hanna Björkelund and Karl Andersson (Uppsala University, Uppsala, Sweden and Ridgeview Instruments AB, Uppsala, Sweden) for technical advices and assistance. Conceived and designed the experiments: DY, NM, ME. Performed the experiments and analyzed the data: DY, CJ, JL, BN. Wrote the paper: DY, FE, ME. All authors read and approved the final version of the manuscript.

GRANT SUPPORT

The Swedish Children Cancer Foundation (PROJ08/006 and PROJ10/027), the Swedish Cancer Society (Contracts 10-0105 and 10-0552), Gunnar Nilsson Cancer Foundation (Grant 65/09) and the Swedish Research Council (Grant K2008-68X-15270-04-3) supported this work.

REFERENCES

1. **Alba, R., A. C. Bradshaw, A. L. Parker, D. Bhella, S. N. Waddington, S. A. Nicklin, N. van Rooijen, J. Custers, J. Goudsmit, D. H. Barouch, J. H. McVey, and A. H. Baker.** 2009. Identification of coagulation factor (F)X binding sites on the adenovirus serotype 5 hexon: effect of mutagenesis on FX interactions and gene transfer. Blood **114:**965-71.
2. **Bauerschmitz, G. J., A. Kanerva, M. Wang, I. Herrmann, D. R. Shaw, T. V. Strong, R. Desmond, D. T. Rein, P. Dall, D. T. Curiel, and A. Hemminki.** 2004. Evaluation of a selectively oncolytic adenovirus for local and systemic treatment of cervical cancer. Int J Cancer **111:**303-9.
3. **Bjorke, H., and K. Andersson.** 2006. Automated, high-resolution cellular retention and uptake studies in vitro. Appl Radiat Isot **64:**901-5.
4. **Boulanger, P. A., and F. Puvion.** 1973. Large-scale preparation of soluble adenovirus hexon, penton and fiber antigens in highly purified form. Eur J Biochem **39:**37-42.
5. **Bridle, B. W., K. B. Stephenson, J. E. Boudreau, S. Koshy, N. Kazdhan, E. Pullenayegum, J. Brunelliere, J. L. Bramson, B. D. Lichty, and Y. Wan.** 2010. Potentiating cancer immunotherapy using an oncolytic virus. Mol Ther **18:**1430-9.
6. **Carlsson, B., W. S. Cheng, T. H. Totterman, and M. Essand.** 2003. Ex vivo stimulation of cytomegalovirus (CMV)-specific T cells using CMV pp65-modified dendritic cells as stimulators. Br J Haematol **121:**428-38.
7. **Cheng, W. S., R. Kraaij, B. Nilsson, L. van der Weel, C. M. de Ridder, T. H. Totterman, and M. Essand.** 2004. A novel TARP-promoter-based adenovirus against hormone-dependent and hormone-refractory prostate cancer. Mol Ther **10:**355-64.
8. **Corjon, S., A. Wortmann, T. Engler, N. van Rooijen, S. Kochanek, and F. Kreppel.** 2008. Targeting of adenovirus vectors to the LRP receptor family with the high-affinity ligand RAP via combined genetic and chemical modification of the pIX capsomere. Mol Ther **16:**1813-24.
9. **Danielsson, A., H. Dzojic, B. Nilsson, and M. Essand.** 2008. Increased therapeutic efficacy of the prostate-specific oncolytic adenovirus Ad[I/PPT-E1A] by reduction of the insulator size and introduction of the full-length E3 region. Cancer gene therapy **15:**203-13.
10. **Danielsson, A., G. Elgue, B. M. Nilsson, B. Nilsson, J. D. Lambris, T. H. Totterman, S. Kochanek, F. Kreppel, and M. Essand.** 2010. An ex vivo loop system models the toxicity and efficacy of PEGylated and unmodified adenovirus serotype 5 in whole human blood. Gene Ther **17:**752-62.
11. **Eiriksdottir, E., K. Konate, U. Langel, G. Divita, and S. Deshayes.** 2010. Secondary structure of cell-penetrating peptides controls membrane interaction and insertion. Biochim Biophys Acta **1798:**1119-28.
12. **El-Andaloussi, S., T. Holm, and U. Langel.** 2005. Cell-penetrating peptides: mechanisms and applications. Curr Pharm Des **11:**3597-611.
13. **Ellis, L. M., S. Samuel, and E. Sceusi.** Varying opinions on the authenticity of a human midgut carcinoid cell line--letter. Clin Cancer Res **16:**5365-6.
14. **Essand, M., J. Leja, V. Giandomenico, and K. E. Oberg.** 2011. Oncolytic Viruses for the Treatment of Neuroendocrine Tumors. Horm Metab Res. doi: 10.1055/s-0031-1277225.
15. **Eto, Y., Y. Yoshioka, R. Asavatanabodee, S. Kida, M. Maeda, Y. Mukai, H. Mizuguchi, K. Kawasaki, N. Okada, and S. Nakagawa.** 2009. Transduction of adenovirus vectors modified with cell-penetrating peptides. Peptides **30:**1548-52.

16. **Fallaux, F. J., O. Kranenburg, S. J. Cramer, A. Houweling, H. Van Ormondt, R. C. Hoeben, and A. J. Van Der Eb.** 1996. Characterization of 911: a new helper cell line for the titration and propagation of early region 1-deleted adenoviral vectors. Hum Gene Ther **7:**215-22.
17. **Franqueville, L., P. Henning, M. Magnusson, E. Vigne, G. Schoehn, M. E. Blair-Zajdel, N. Habib, L. Lindholm, G. E. Blair, S. S. Hong, and P. Boulanger.** 2008. Protein crystals in Adenovirus type 5-infected cells: requirements for intranuclear crystallogenesis, structural and functional analysis. PLoS One **3:**e2894.
18. **Froidevaux, S., and F. Loor.** 1991. A quick procedure for identifying doubly homozygous immunodeficient scid beige mice. J Immunol Methods **137:**275-9.
19. **Fueyo, J., C. Gomez-Manzano, R. Alemany, P. S. Lee, T. J. McDonnell, P. Mitlianga, Y. X. Shi, V. A. Levin, W. K. Yung, and A. P. Kyritsis.** 2000. A mutant oncolytic adenovirus targeting the Rb pathway produces anti-glioma effect in vivo. Oncogene **19:**2-12.
20. **Fukazawa, T., J. Matsuoka, T. Yamatsuji, Y. Maeda, M. L. Durbin, and Y. Naomoto.** 2010. Adenovirus-mediated cancer gene therapy and virotherapy (Review). Int J Mol Med **25:**3-10.
21. **Geoerger, B., V. W. van Beusechem, P. Opolon, J. Morizet, L. Laudani, Y. Lecluse, M. Barrois, S. Idema, J. Grill, W. R. Gerritsen, and G. Vassal.** 2005. Expression of p53, or targeting towards EGFR, enhances the oncolytic potency of conditionally replicative adenovirus against neuroblastoma. J Gene Med **7:**584-94.
22. **Kreppel, F., J. Gackowski, E. Schmidt, and S. Kochanek.** 2005. Combined genetic and chemical capsid modifications enable flexible and efficient de- and retargeting of adenovirus vectors. Mol Ther **12:**107-17.
23. **Kurachi, S., K. Tashiro, F. Sakurai, H. Sakurai, K. Kawabata, K. Yayama, H. Okamoto, S. Nakagawa, and H. Mizuguchi.** 2007. Fiber-modified adenovirus vectors containing the TAT peptide derived from HIV-1 in the fiber knob have efficient gene transfer activity. Gene Ther **14:**1160-5.
24. **Lambert, C., N. Leonard, X. De Bolle, and E. Depiereux.** 2002. ESyPred3D: Prediction of proteins 3D structures. Bioinformatics **18:**1250-6.
25. **Leifert, J. A., S. Harkins, and J. L. Whitton.** 2002. Full-length proteins attached to the HIV tat protein transduction domain are neither transduced between cells, nor exhibit enhanced immunogenicity. Gene Ther **9:**1422-8.
26. **Leja, J., H. Dzojic, E. Gustafson, K. Oberg, V. Giandomenico, and M. Essand.** 2007. A novel chromogranin-A promoter-driven oncolytic adenovirus for midgut carcinoid therapy. Clin Cancer Res **13:**2455-62.
27. **Leja, J., B. Nilsson, D. Yu, E. Gustafson, G. Akerstrom, K. Oberg, V. Giandomenico, and M. Essand.** 2010. Double-detargeted oncolytic adenovirus shows replication arrest in liver cells and retains neuroendocrine cell killing ability. PLoS One **5:**e8916.
28. **Leja, J., D. Yu, B. Nilsson, L. Gedda, A. Zieba, T. Hakkarainen, G. Akerstrom, K. Oberg, V. Giandomenico, and M. Essand.** 2011. Oncolytic adenovirus modified with somatostatin motifs for selective infection of neuroendocrine tumor cells. Gene Ther. doi: 10.1038/gt.2011.54.
29. **Parikh, N. S., M. A. Currier, Y. Y. Mahller, L. C. Adams, B. Di Pasquale, M. H. Collins, and T. P. Cripe.** 2005. Oncolytic herpes simplex virus mutants are more efficacious than wild-type adenovirus Type 5 for the treatment of high-risk neuroblastomas in preclinical models. Pediatr Blood Cancer **44:**469-78.
30. **Pesonen, S., P. Nokisalmi, S. Escutenaire, M. Sarkioja, M. Raki, V. Cerullo, L. Kangasniemi, L. Laasonen, C. Ribacka, K. Guse, E. Haavisto, M. Oksanen, M. Rajecki, A.**

Helminen, A. Ristimaki, A. Karioja-Kallio, E. Karli, T. Kantola, G. Bauerschmitz, A. Kanerva, T. Joensuu, and A. Hemminki. 2010. Prolonged systemic circulation of chimeric oncolytic adenovirus Ad5/3-Cox2L-D24 in patients with metastatic and refractory solid tumors. Gene Ther **17:**892-904.

31. **Rebetz, J., M. Na, C. Su, B. Holmqvist, A. Edqvist, C. Nyberg, B. Widegren, L. G. Salford, H. O. Sjogren, N. Arnberg, Q. Qian, and X. Fan.** 2009. Fiber mediated receptor masking in non-infected bystander cells restricts adenovirus cell killing effect but promotes adenovirus host co-existence. PLoS One **4:**e8484.

32. **Roberts, D. M., A. Nanda, M. J. Havenga, P. Abbink, D. M. Lynch, B. A. Ewald, J. Liu, A. R. Thorner, P. E. Swanson, D. A. Gorgone, M. A. Lifton, A. A. Lemckert, L. Holterman, B. Chen, A. Dilraj, A. Carville, K. G. Mansfield, J. Goudsmit, and D. H. Barouch.** 2006. Hexon-chimaeric adenovirus serotype 5 vectors circumvent pre-existing anti-vector immunity. Nature **441:**239-43.

33. **Rux, J. J., P. R. Kuser, and R. M. Burnett.** 2003. Structural and phylogenetic analysis of adenovirus hexons by use of high-resolution x-ray crystallographic, molecular modeling, and sequence-based methods. J Virol **77:**9553-66.

34. **Sawant, R., and V. Torchilin.** 2010. Intracellular transduction using cell-penetrating peptides. Mol Biosyst **6:**628-40.

35. **Schaeffer, C., and M. A. Warso.** 2009. A Phase I Trial of p28 (Cell Penetrating Peptide) in the Treatment of Refractory Solid Tumors. http://clinicaltrials.gov/ct2/show/NCT00914914.

36. **Seregin, S. S., and A. Amalfitano.** 2009. Overcoming pre-existing adenovirus immunity by genetic engineering of adenovirus-based vectors. Expert Opin Biol Ther **9:**1521-31.

37. **Shashkova, E. V., S. M. May, K. Doronin, and M. A. Barry.** 2009. Expanded anticancer therapeutic window of hexon-modified oncolytic adenovirus. Mol Ther **17:**2121-30.

38. **Stanton, R. J., B. P. McSharry, M. Armstrong, P. Tomasec, and G. W. Wilkinson.** 2008. Re-engineering adenovirus vector systems to enable high-throughput analyses of gene function. Biotechniques **45:**659-62, 664-8.

39. **Terao, S., B. Acharya, T. Suzuki, T. Aoi, M. Naoe, K. Hamada, H. Mizuguchi, and A. Gotoh.** 2009. Improved gene transfer into renal carcinoma cells using adenovirus vector containing RGD motif. Anticancer Res **29:**2997-3001.

40. **Thomas, M. A., D. L. Lichtenstein, P. Krajcsi, and W. S. Wold.** 2007. A real-time PCR method to rapidly titer adenovirus stocks. Methods Mol Med **130:**185-92.

41. **Thorne, S. H., W. Liang, P. Sampath, T. Schmidt, R. Sikorski, A. Beilhack, and C. H. Contag.** 2010. Targeting localized immune suppression within the tumor through repeat cycles of immune cell-oncolytic virus combination therapy. Mol Ther **18:**1698-705.

42. **Tollefson, A. E., M. Kuppuswamy, E. V. Shashkova, K. Doronin, and W. S. Wold.** 2007. Preparation and titration of CsCl-banded adenovirus stocks. Methods Mol Med **130:**223-35.

43. **Van Buren, G., 2nd, A. Rashid, A. D. Yang, E. K. Abdalla, M. J. Gray, W. Liu, R. Somcio, F. Fan, E. R. Camp, J. C. Yao, and L. M. Ellis.** 2007. The development and characterization of a human midgut carcinoid cell line. Clin Cancer Res **13:**4704-12.

44. **Vellinga, J., J. de Vrij, S. Myhre, T. Uil, P. Martineau, L. Lindholm, and R. C. Hoeben.** 2007. Efficient incorporation of a functional hyper-stable single-chain antibody fragment protein-IX fusion in the adenovirus capsid. Gene Ther **14:**664-70.

45. **Vigant, F., D. Descamps, B. Jullienne, S. Esselin, E. Connault, P. Opolon, T. Tordjmann, E. Vigne, M. Perricaudet, and K. Benihoud.** 2008. Substitution of hexon hypervariable

region 5 of adenovirus serotype 5 abrogates blood factor binding and limits gene transfer to liver. Mol Ther **16:**1474-80.

46. **Vigne, E., I. Mahfouz, J. F. Dedieu, A. Brie, M. Perricaudet, and P. Yeh.** 1999. RGD inclusion in the hexon monomer provides adenovirus type 5-based vectors with a fiber knob-independent pathway for infection. J Virol **73:**5156-61.

47. **Waddington, S. N., J. H. McVey, D. Bhella, A. L. Parker, K. Barker, H. Atoda, R. Pink, S. M. Buckley, J. A. Greig, L. Denby, J. Custers, T. Morita, I. M. Francischetti, R. Q. Monteiro, D. H. Barouch, N. van Rooijen, C. Napoli, M. J. Havenga, S. A. Nicklin, and A. H. Baker.** 2008. Adenovirus serotype 5 hexon mediates liver gene transfer. Cell **132:**397-409.

48. **Wang, H., Z. Y. Li, Y. Liu, J. Persson, I. Beyer, T. Moller, D. Koyuncu, M. R. Drescher, R. Strauss, X. B. Zhang, J. K. Wahl, 3rd, N. Urban, C. Drescher, A. Hemminki, P. Fender, and A. Lieber.** 2011. Desmoglein 2 is a receptor for adenovirus serotypes 3, 7, 11 and 14. Nat Med **17:**96-104.

49. **Wang, H., Y. C. Liaw, D. Stone, O. Kalyuzhniy, I. Amiraslanov, S. Tuve, C. L. Verlinde, D. Shayakhmetov, T. Stehle, S. Roffler, and A. Lieber.** 2007. Identification of CD46 binding sites within the adenovirus serotype 35 fiber knob. J Virol **81:**12785-92.

50. **Wu, H., T. Han, N. Belousova, V. Krasnykh, E. Kashentseva, I. Dmitriev, M. Kataram, P. J. Mahasreshti, and D. T. Curiel.** 2005. Identification of sites in adenovirus hexon for foreign peptide incorporation. J Virol **79:**3382-90.

51. **Yoshioka, Y., R. Asavatanabodee, Y. Eto, H. Watanabe, T. Morishige, X. Yao, S. Kida, M. Maeda, Y. Mukai, H. Mizuguchi, K. Kawasaki, N. Okada, and S. Nakagawa.** 2008. Tat conjugation of adenovirus vector broadens tropism and enhances transduction efficiency. Life Sci **83:**747-55.

52. **Zhang, Y. Q., Y. C. Tsai, A. Monie, T. C. Wu, and C. F. Hung.** 2010. Enhancing the therapeutic effect against ovarian cancer through a combination of viral oncolysis and antigen-specific immunotherapy. Mol Ther **18:**692-9.

Figure Legends

Figure 1. Illustration of the Ad5 recombineering strategy, predicted structure of hexon with Tat-PTD, a schematic drawing and titers of the viruses used. (**a**) An illustration of the selection-counter selection steps used for recombineering of Ad5 with the bacteriophage λ-Red system. In the first selection step, the *als* (Amp-LacZ-SacB)-cassette is PCR amplified with primers that introduce 50 bp of homologous sequence to the virus genome on each side of the site of modification (in this case HVR5). The PCR product containing the *als*-cassette is inserted into the modification site and the selection is based on ampicillin resistance and blue colonies. In the second counter-selection step, a PCR product is generated with the desired modification (in this case insertion of Tat-PTD) with flanking sequences of 50 bp with homology to the virus genome on each side of the site of modification. The *als*-cassette is replaced by the desired sequence and the selection is based on sucrose and white colonies. A scarless modification has been introduced. (**b**) The predicted model shows the side view of a trimerized hexon with Tat-PTD in red (Trace) and α-helix spacer in cyan (Ribbon) in HVR5. The prediction was based on the online software tool (ESyPred3D Web Server 1.0), to which the amino acid sequence with the Tat-PTD modification was sent and the original hexon structure (PDB: 1P30) was selected as a template for the prediction. The software automatically gives out the prediction structure. (**c**) Illustration of the recombinant viruses used in this study. (**d**) Titers of the viruses used in the study.

Figure 2. A Tat-PTD-modified Ad5 vector can transduce cells with low CAR expression. Cells were transduced in suspension for 2 hours with GFP-expressing adenoviral vectors at various evg/cell. The viral vector was then washed away and the cells were analyzed by flow cytometry 48 hours after transduction. Values are shown as mean+SD from three independent experiments, each with triplicate samples. Unpaired Student's *t*-test was used for comparison (***: $p<0.001$; not significant (n.s.): $p>0.05$; n=3). The values in parenthesis after each cell line name indicate the CAR expression level (percentage of CAR positive cells) as assessed by FACS staining.

Figure 3. Tat-PTD-modified oncolytic adenoviruses yield enhanced cell killing and replication activities. (**a**) A neuroblastoma (SK-N-SH) and a neuroendocrine tumor (CNDT2.5) cell lines, both with low CAR expression, were transduced with Tat-PTD-modified or wild type Ad5 virus at various evg/cell. The non-replication-competent Tat-PTD-modified viral vector Ad5PTD(GFP) was used as a negative control. The relative cell viability was analyzed 4 days after transduction by MTS assay. Data are shown as mean±SD from three independent experiments, each with triplicate samples (***: $p<0.001$; n=3). (**b**) Neuroblastoma (SK-N-SH) cells were transduced with virus at 500 evg/cell. Viral genomic DNA was isolated at day 0, 1, 2, 3 after transduction and quantified using real-time PCR. Values show the fold change in relation to day 0 (set to 1). Data is shown as mean±SD from three independent experiments, each with triplicate samples (***: $p<0.001$; n=3). (**c**) SK-N-SH cells were transduced with virus at 500 evg/cell. Total protein lysates were prepared after 48 hours and 50 µg of samples were resolved

by SDS-PAGE. E1A was detected by Western blotting using an anti-E1A antibody. β-Actin was used as loading control.

Figure 4. A Tat-PTD-modified oncolytic adenovirus overcomes the fiber-masking problem and spreads more efficiently than a non-modified virus. (**a**) A549 cells were transduced with GFP-expressing adenoviral vectors at 500 evg/cell in the presence of free soluble Ad5 fiber molecules and analyzed by flow cytometry after 2 days. Transduced cells in the absence of soluble Ad5 fiber served as control (set to 100%) (***: $p<0.001$; n=3). (**b**) Monolayer A549 cells were transduced with equal amount of either Ad5(wt) or Ad5PTD(wt) followed by low-melting agar overlay and neutral red staining. Plaque sizes measured after 8 days are represented as whisker box-plot with median, lower quartile, upper quartile, minimum and maximum values. Comparison was performed by the non-parametric Mann-Whitney test (***: $p<0.001$, n=50). (**c**) Representative images of the whole well from the plaque formation assay at day 8, formed by Ad5(wt) and Ad5PTD(wt). 10X magnification pictures were shown accordingly as well.

Figure 5. Tat-PTD-modified Ad5 vector can resist FX-mediated uptake and partially overcome anti-Ad5 antibodies. (**a**) 5000 evg of either FITC-labeled Ad5(wt) or FITC-labeled Ad5PTD(wt) in 3mL of culture medium was added to monolayer SKOV3 cells, covering a small portion of the culture dish, in the presence or absence of FX (8μg/mL). The FX-mediated virus-cell binding interaction was measured and recorded in real-time

by LigandTracer® Green. Representative data from one experiment out of three is shown. (**b**) Monolayer SKOV3 cells were transduced for 1 hour at 4°C with GFP-expressing adenoviral vectors at 500 evg/cell in the presence of FX (8μg/mL). Transduced cells without the addition of FX served as control (set to 100%). Viral genomic DNA was isolated directly after transduction and quantified by real-time PCR. Representative data from one experiment out of two is shown. (**c**) A549 cells were transduced with GFP-expressing adenoviral vectors at 500 evg/cell in the presence of heat-inactivated mouse plasma, from mice immunized with Ad5(mock), at various dilutions and analyzed by flow cytometry after 24 hours. Transduced cells in the absence of mouse serum served as control (set to 100%). Data are presented as mean+SD from at least three independent experiments, each with triplicate samples. Student's t-test was performed for statistical differences (***: $p<0.001$; *: $p<0.05$; n.s.: $p>0.05$).

Figure 6. Treatment with Tat-PTD-modified oncolytic adenoviruses delay tumor growth and prolong survival in mice with transplanted human neuroblastoma and neuroendocrine tumors. (**a**) SCID/beige mice harboring subcutaneous neuroblastoma, SK-N-SH, were treated by peritumoral virus injections as indicated by the arrows. (**c**) NMRI-nude mice harboring subcutaneous neuroendocrine tumor, CNDT2.5, were treated by intratumoral virus injections as indicated by arrows. The tumor volume was monitored by caliper measurements. Six mice per group were used and data is shown as mean+SD. Mice were sacrificed when the tumor size reached 800 mm^3. The experiment of SCID/beige mice was terminated when the last mouse in the Ad5(wt)-treatment

group was sacrificed due to wounds on the tumors. The experiment of NMRI-nude was terminated at day 100 after tumor implantation. A Kaplan-Meier survival curve shows survival data (**b**, SCID/beige mice; **d**, NMRI-nude mice). Log-rank test was performed for comparison.

Table 1. List of primers used in this study

Primer name	Sequences (5'-3')
pF.Shuni	GATTTGGCCATTTTCGCGGG
pR.Shuni	GGCGGCTGCTGCAAAACAGAT
pF.HVR5-als	AATGGAAAGCTAGAAAGTCAAGTGGAAATGCAATTTTTCCC TGTGACGGAAGATCACTTCG
pR.HVR5-als	CCACTTTAGGAGTCAAGTTATCACCATTGCCTGCGGCTGCC TGAGGTTCTTATGGCTCTTG
pF.E1-als	CTGAATAAGAGGAAGTGAAATCTGAATAATTTTGTGTTACT CATAGCGCG*GGATCC*CCTGTGACGGAAGATC
pR.E1-als	GATACAAAACTACATAAGACCCCCACCTTATATATTCTTTC CCACCC*GGATCC*CTGAGGTTCTTATGGC
pF1.HVR5-PTD	CCCCAATGAAACCATGTTAC
pR1.HVR5-PTD	**TCTTCGTCGCTGTCTCCGCTTCTTCCTGCCATATCCACCTC CAGCTCCACCTCCAGC**AGTAGTTGAGAAAAATTGCA
pF2.HVR5-PTD	**TATGGCAGGAAGAAGCGGAGACAGCGACGAAGAGGAGGTGG AGCTGGAGGTGGAGCT**ACTCCTAAAGTGGTATTGTAC
pR2.HVR5-PTD	GCAATGTAATTAGGCCTGTTG
Ad.Titration.F	CATCAGGTTGATTCACATCGG
Ad.Titration.R	GAAGCGCTGTATGTTGTTCTG

Sequences with homologous region are underlined. PTD modification sequences are **bold**. Restriction sites are *italic*.

Figure 1

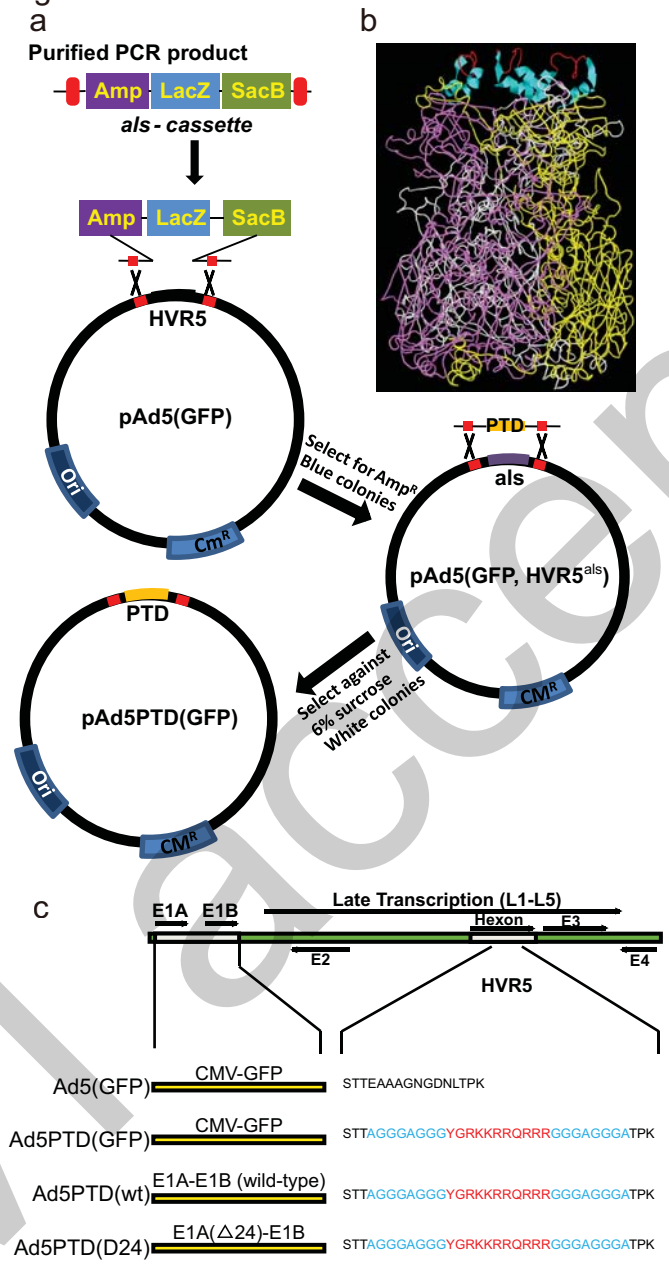

d

Viruses	evg/μL	FFU/μL	evg/FFU
Ad5(mock)	2.9×10^{8}	1.0×10^{7}	29.0
Ad5(GFP)	5.4×10^{8}	3.7×10^{7}	14.6
Ad5PTD(GFP)	1.1×10^{9}	9.9×10^{7}	11.1
Ad5(wt)	2.6×10^{9}	7.0×10^{7}	37.1
Ad5PTD(wt)	8.2×10^{8}	4.9×10^{7}	16.7
Ad5PTD(D24)	8.6×10^{8}	8.0×10^{7}	10.8

Figure 2

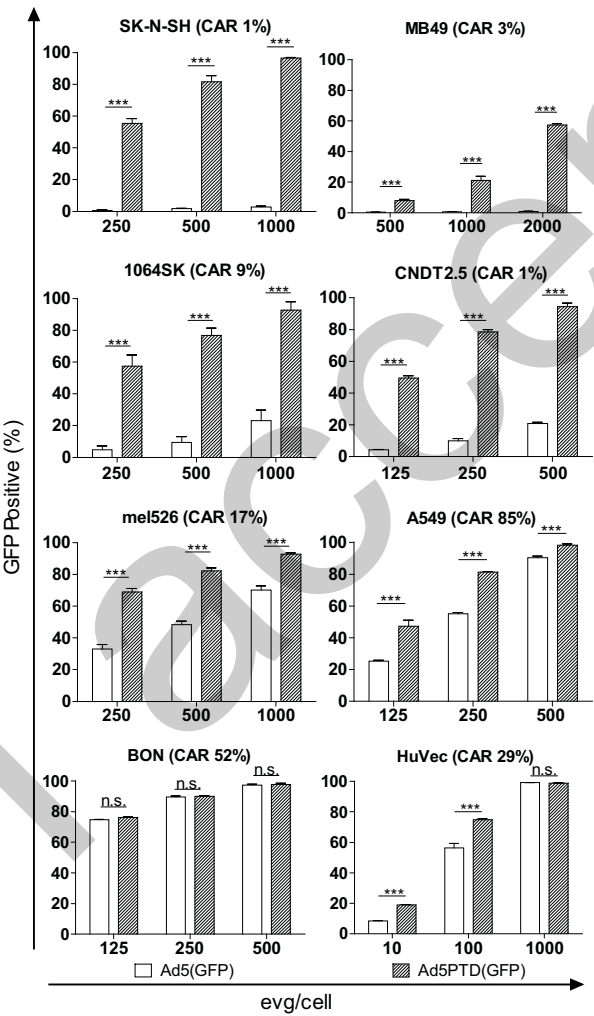
SK-N-SH (CAR 1%)
MB49 (CAR 3%)
1064SK (CAR 9%)
CNDT2.5 (CAR 1%)
mel526 (CAR 17%)
A549 (CAR 85%)
BON (CAR 52%)
HuVec (CAR 29%)
GFP Positive (%)
***
n.s.
250
500
1000
2000
125
10
100
Ad5(GFP)
Ad5PTD(GFP)
evg/cell

Figure 3

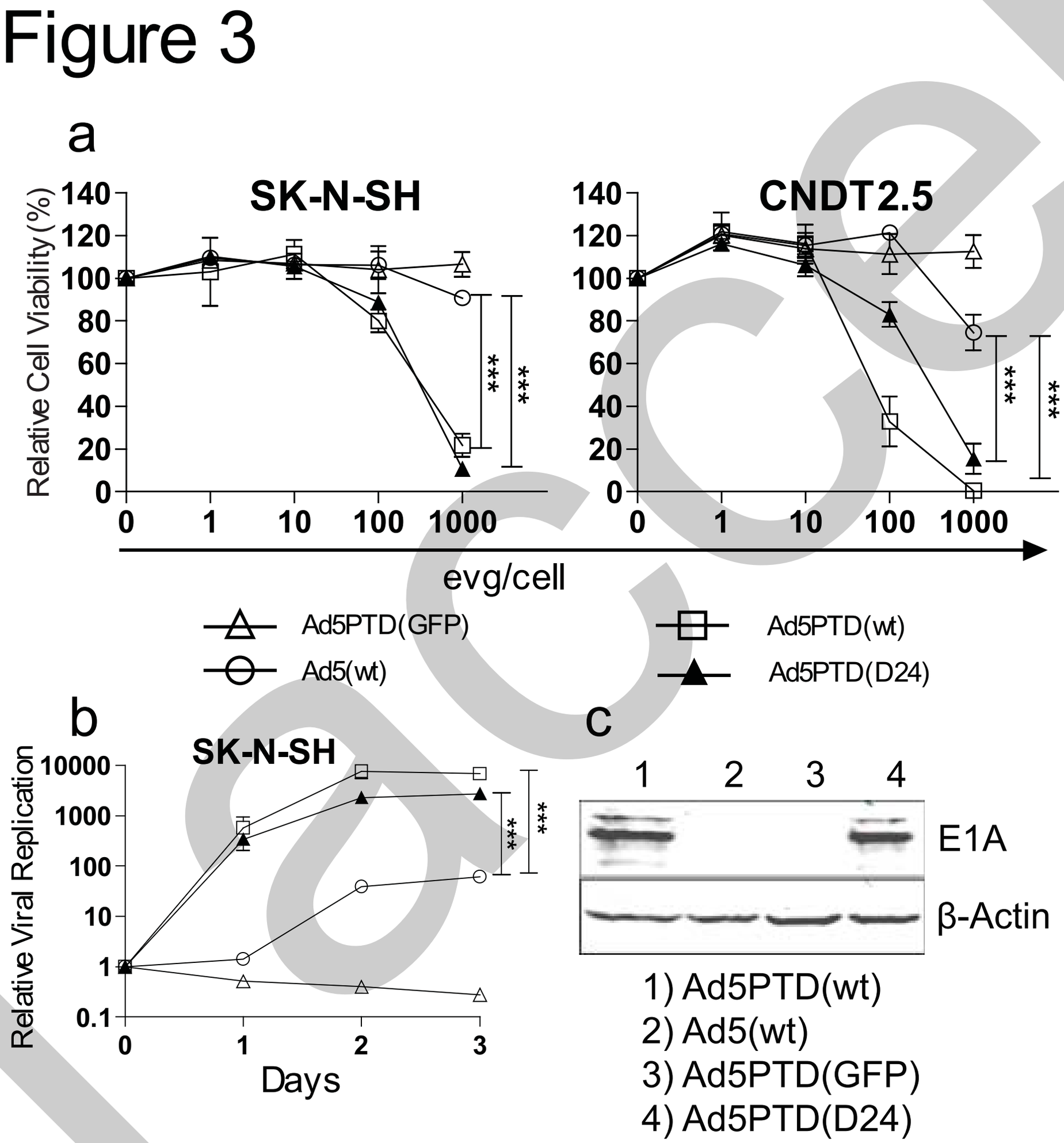
a
SK-N-SH
CNDT2.5
Relative Cell Viability (%)
140
120
100
80
60
40
20
0
0
1
10
100
1000
evg/cell
***
***
***
***
Ad5PTD(GFP)
Ad5(wt)
Ad5PTD(wt)
Ad5PTD(D24)
b
SK-N-SH
Relative Viral Replication
10000
1000
100
10
1
0.1
0
1
2
3
Days
***
***
c
1
2
3
4
E1A
β-Actin
1) Ad5PTD(wt)
2) Ad5(wt)
3) Ad5PTD(GFP)
4) Ad5PTD(D24)

Figure 4

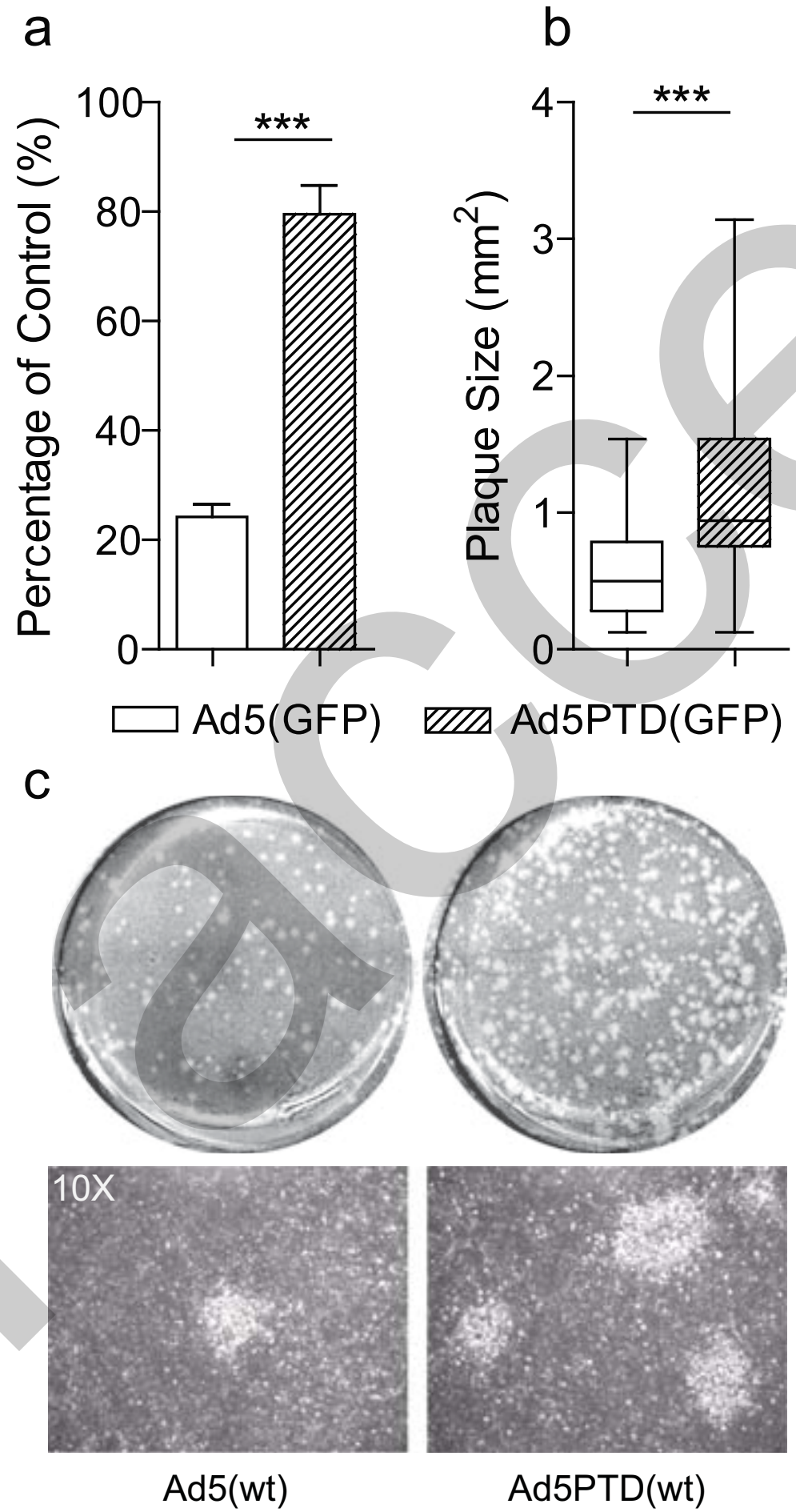
a
b
c
Percentage of Control (%)
100
80
60
40
20
0
***
Plaque Size (mm2)
4
3
2
1
0
***
Ad5(GFP)
Ad5PTD(GFP)
10X
Ad5(wt)
Ad5PTD(wt)

Figure 5

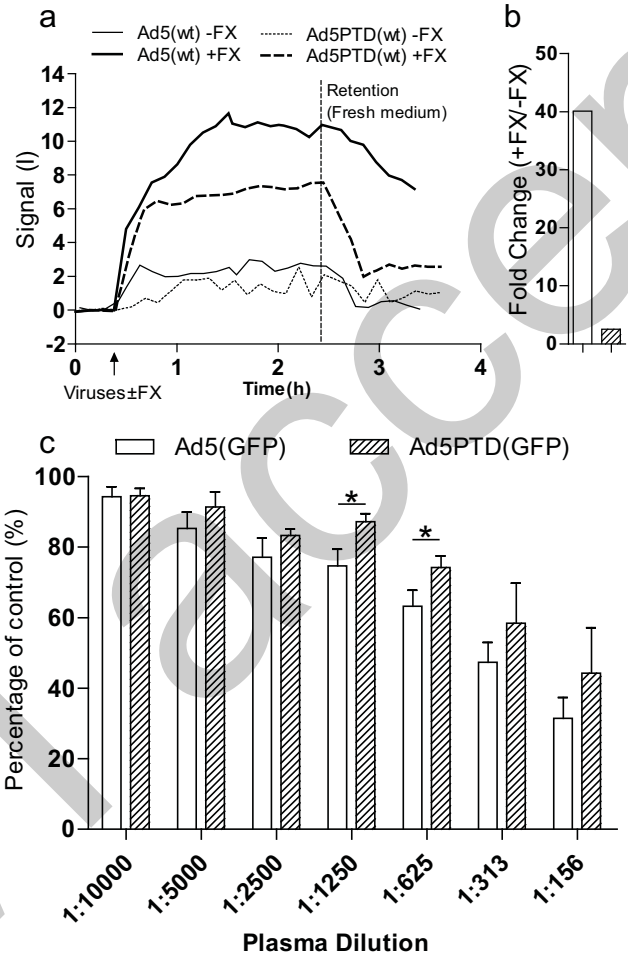
a
Ad5(wt) -FX
Ad5(wt) +FX
Ad5PTD(wt) -FX
Ad5PTD(wt) +FX
Retention
(Fresh medium)
Signal (I)
Viruses±FX
Time(h)
b
Fold Change (+FX/-FX)
c
Ad5(GFP)
Ad5PTD(GFP)
Percentage of control (%)
1:10000
1:5000
1:2500
1:1250
1:625
1:313
1:156
Plasma Dilution

Figure 6